Microwave photodielectric and photoconductivity studies on titanium dioxide exposed to continuous, polychromatic irradiation Part I: A novel analytical tool to assess the photoactivity of titanium dioxide

Michele Edge [a,*], Robert Janes [a], Julie Robinson [a], Norman Allen [a] Frank Thompson [a], John Warman [b]

[a] Department of Chemistry, the Manchester Metropolitan University, Chester Street, Manchester M1 5GD, UK
[b] Radiation Chemistry Department, IRI, Delft University of Technology, Mekelweg 15, 2696 JB Delft, Netherlands

Abstract

A novel analytical method is described which allows the charge-carrier dynamics taking place when titanium dioxide is subjected to ultrabandgap irradiation to be measured. Samples are exposed continuously to polychromatic light and photophysical processes monitored in real-time. The method relies on the perturbations that take place in the stored energy characteristics of a microwave cavity. In such a device, the electric and magnetic fields of the microwave energy reach a maximum when they are resonant with the cavity. Titanium dioxide powders held in the cavity, and simultaneously irradiated with visible light, produce free-carriers which reduce the stored energy density of the cavity. This results in a shift in the value of the resonant frequency and an attenuation of the microwave power, which are in proportion to the population of free-carriers produced in the sample. The frequency measurements are tempered by the presence of localised (trapped) carriers. Uncoupling the changes in power and frequency allows the dynamics of free and trapped carriers to be quantified. The results derived from this real-time method are consistent with those reported from time-resolved microwave conductivity (TRMC) measurements, which follow the decay of conductivity following a pulse of high intensity light. In addition, the real-time method follows the build-up of charge-carriers during irradiation as well as their decay immediately after irradiation. Data is presented for anatase, rutile and a sample of mixed morphology (75% anatase:25% rutile). The influences of sample size, humidity, temperature, light-intensity and wavelength on the microwave response, are considered.   © 1998 Elsevier Science S.A.

Keywords: Titanium dioxide; Polychromatic irradiation; Photoactivity

1. Introduction

Two groups of chemists are interested in the photoactivity of titanium dioxide: polymer chemists want to minimise the photoactivity in paints and coatings [1], and photochemists wish to maximise it [2]. To suppress photoactivity, the fast recombination of charge-carriers and the inhibition of interfacial charge-transfer are necessary. Conversely, to enhance photocatalytic activity inhibition of recombination processes and efficient interfacial charge-transfer are required. To distinguish these processes, we need a simple and direct method of probing charge-carrier dynamics in practical systems.

Microwave cavity perturbation methods offer an advantage over many techniques, in that they are contactless. As

such, they do not mask interfacial process by generating the surface contact potentials from which DC methods suffer [3]. Furthermore, the sensitivity of microwave methods allows us to monitor charge transport in materials that produce carriers of low mobility. The microwave method adapted for use in this study employs a resonance technique [4–8]. The microwaves are directed via a waveguide, through an aperture into a cavity. At most microwave frequencies, there is very little penetration of microwaves into the empty cavity, but at certain frequencies, the cavity abstracts appreciable power (i.e., microwaves oscillate between electric and magnetic fields reaching a maximum when they are resonant with the cavity).

When a sample is placed in the microwave cavity, the alternating field gives rise to dielectric dispersion (i.e., the characteristic (orientation) motions of dipoles result in a frequency variation of the dielectric constant of the sample,

* Corresponding author.

and the appearance of 'dielectric loss' over a broad range of frequencies) [9]. When the direction of the field is changing sufficiently fast, the forces impeding the dipole orientation are dominant, and the dipoles are unable to follow the changes. At these frequencies, the orientation of permanent dipoles no longer contributes to the dielectric constant. At certain frequencies, energy drawn from the cavity is dissipated as heat. This reduces the ability of the cavity to store energy and hence, microwave power is attenuated and the resonant frequency shifts to a lower value.

These interactions give rise to a complex susceptibility of the dielectric constant of the sample. Because dielectric loss describes the motion of electric charge, it is to the imaginary part of the dielectric constant that conductivity processes contribute. In the case of photoconductors, conduction arises not from the affect of polarisation on the displacement current, but from actual charge-transport. Normally, such conduction would be described by a volume conductivity, the effect of which is to add an additional term to the dielectric loss. Hence, the energy stored by a microwave cavity is reduced further when free-carriers are produced. The free-carriers absorb microwave energy creating large numbers of phonons, further reducing the stored energy density of the cavity, the resulting attenuation of microwave power being in proportion to the number of free-carriers produced.

The real part of the susceptibility represents the dielectric constant (i.e., a measure of the extent to which the electric charge distribution in the sample can be distorted or polarised by the application of the electric field). Trapped carriers respond to the alternating microwave field and so, have relatively little affect on stored energy density (though it should be noted that the depth of trapping is important since shallowly trapped carriers may contribute to conductivity). However, they do give rise to polarisable centres that alter the value of the microwave cavity resonant frequency.

The majority of microwave methods described in the literature monitor only the conductivity component of dielectric loss. The methods given are time-resolved and measure transient states. To achieve this, they employ high-energy sources (lasers, electron pulses) to generate a sufficient population of free-carriers. It is unfortunate that this tends to promote direct recombination of carriers over trap related decay. In contrast, the present study uses a polychromatic light source and follows the build-up of carriers (during irradiation) and their decay (on removal of the light source) in real-time. In this context, the present study evaluates the potential of the real-time microwave method and its limitations.

2. Experimental

To produce a measurable microwave response, two aspects of equipment design were necessary: (1) The construction of a rectangular waveguide with a cylindrical cavity that could house powdered samples in such a way as to maximise the surface area exposed to the light source (Fig. 1). To ensure
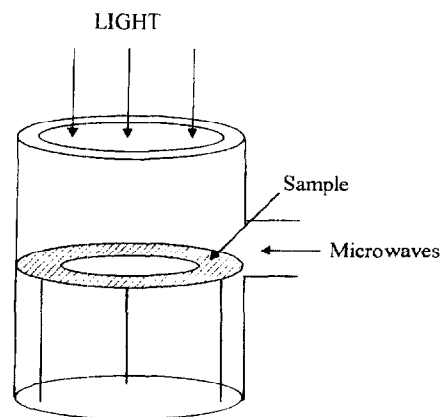
LIGHT

Fig. 1. The irradiation configuration of the microwave cavity used for real-time measurements.

reproducibility of packing of the powders in the sample holder, a vibrator was used (it should be noted here that even though the cavity design was optimised to evaluate the photoactivity of powders, it is possible to modify the cavity to enable measurements on colloidal dispersions of TiO_2 powders or a pigmented, polymer matrix). (2) The use of a light-source, which could generate sufficient carriers in the sample, which in turn would produce a measurable, microwave response (in consideration of the wide range of TiO_2 photoactivities).

Real-time microwave measurements were carried out using a Marconi 6310 programmable sweep generator (2–20 GHz) connected via the waveguide to a Marconi 6500 automatic amplitude analyser. Samples were irradiated with polychromatic light from a Rank Aldis projector unit (240 V) with a tungsten filament (Reflecta AF1800) light-source (250 W). The TiO_2 samples (2.0 g, unless specified otherwise) were obtained from Tioxide and Degussa. The TiO_2 samples provided by Tioxide were both uncoated, pigmentary grade samples produced for purity rather than performance. These samples were used in both real-time and time resolved microwave experiments.

The relative humidity of the cavity was modified using saturated aqueous salt solutions of ammonium sulphate, sodium bromide and solid calcium chloride. The cavity and light-source were enclosed using transparent polyethylene sheets, and the relative humidity of the sealed atmosphere was monitored until equilibrium was reached and the cavity resonant frequency located. Samples were equilibrated at 25°C and relative humidity of 30%, 55%, 63% and 73%.

The cavity temperature was controlled by means of a Gallenkamp heater and RS components digital thermometer. For each measurement, the sample was allowed to reach thermal equilibrium for 30 min prior to irradiation.

Light emanating from a monochromator and xenon arc source (150 W) did not produce any measurable photoresponse, consequently, to irradiate over a known wavelength profile, filtered light from the 250 W tungsten lamp was employed. The wavelength of incident light was modified using solution filters consisting of the following media: $CoCl_2$

Table 1

The light intensity emanating from a 250 W tungsten filament source when masked by various solution filters

Filter solution	Light intensity (W)
Water	243
CoCl₃	222
NiSO₄	211
CuSO₄	158
CrCl₃	157
Fe₂(SO₄)₃	208
KMnO₄	117

(0.05 M), NiSO₄ (0.05 M), CuSO₄ (0.05 M), CrCl₃ (0.05 M), Fe₂(SO₄)₃ (0.05 M) and KMnO₄ (0.02 M). The intensity of the light impinging on the sample was measured using a Newport digital power meter (see Table 1). In addition, the light intensity of the 250 W source was varied using a dimmer unit.

The time-resolved measurements were undertaken at Delft University of Technology. TiO_2 powders were compressed by hand into a small cylindrical cavity that fitted a rectangular waveguide. The sample was irradiated with 3 MeV electrons from a Van de Graff accelerator with pulses that could be varied in width from 0.5 to 250 ns and corresponded to energy between 3×10^{-6} and 3 J per pulse. The penetration depth and beam dimensions were such that the sample was considered uniformly irradiated throughout its volume. (Further details of this experimental set-up are given in Ref. [10].)

3. Results and discussion

The main objective of this study was to establish a relationship between the observed dielectric properties monitored by the microwave method with the photoactivity of TiO_2 powders. To achieve this, the photoactivities of anatase, rutile and a sample of mixed-morphology were studied. Photoactivity was determined as a function of several environmental variables (e.g., temperature, humidity).

3.1. The influence of polymorphism on microwave response

In Fig. 2, the resultant trace from the automatic microwave amplitude analyser is presented, showing the attenuation of microwave power and the shift in cavity resonant frequency, for anatase and rutile powders prior to irradiation. The changes in cavity properties in the presence of dielectrics may be rationalised by reference to the work of Hartwig and Hinds [11]. These workers assessed the effect of polarisable, trapped charge centres in irradiated CdS, within the context of microwave cavity perturbation theory. They demonstrated that the cavity resonant frequency should decrease due to an increase in dielectric constant in the presence of localised carriers (electrons). In contrast, delocalised carriers (conduction electrons) produce an increase in cavity resonant
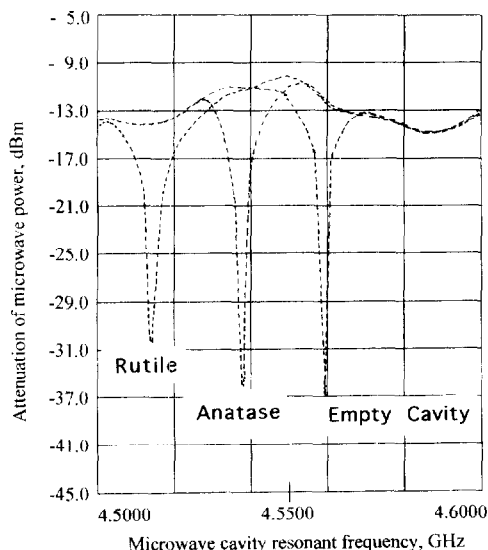

Fig. 2. Microwave resonant absorption maxima for anatase and rutile relative to the empty cavity.
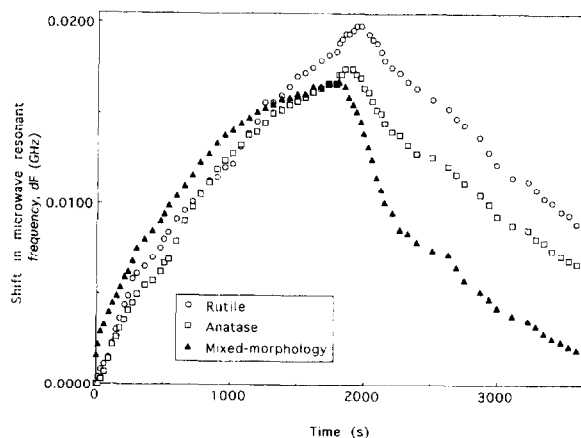

Fig. 3. Shift of microwave cavity resonant frequency for rutile and anatase powders during consecutive periods of light exposure and darkness.

frequency due to a decreased dielectric constant. Fig. 2 illustrates that before irradiation, the shift of resonant frequency to lower values is greater for the rutile sample than for the anatase sample, which is a reflection of the greater polarisability of rutile c.f. anatase (polarisability vol.% for rutile is 0.398 c.f. 0.367 for anatase). The positive shift of dF (Fig. 3) during sample irradiation is a consequence of the dominance of photoproduced free-carriers. However, it should be borne in mind that the relative magnitudes of frequency shift are controlled by the presence of localised centres within the crystal lattice. The differences between the value of the initial frequency shifts of the anatase and rutile samples and the value of the shift after 1800 s of continuous, polychromatic light exposure are 0.0174 GHz and 0.0198 GHz ($\sigma = \pm 0.0004$ GHz), respectively. The lower value for anatase suggests that the extent of frequency shift is tempered by a greater amount of carrier trapping. Continuous, polychromatic irradiation produces ca. 10^{18} carriers cm⁻³ of sample. At this concentration, free-carriers will rapidly saturate the

Table 2

Values of attenuated microwave power and cavity resonant frequency for anatase and rutile powders (prior to irradiation, after 1800 s of continuous exposure, and 1800 s after exposure)

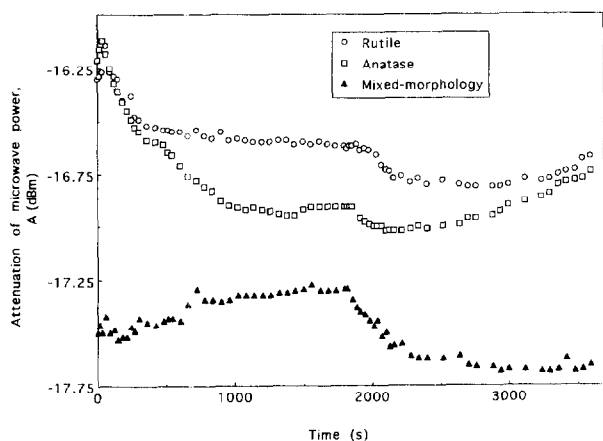|		Anatase	Rutile	Mixed morphology
(1)	Initial power (dBm)	−16.21	−16.30	−17.27
(2)	Power after 1800-s exposure (dBm)	−16.91	−16.64	−17.29
	(2)–(1)	0.70	0.30	0.02
(3)	Final power (dBm)	−16.53	−16.48	−17.62
	(3)–(1)	0.32	0.18	0.35
(4)	Initial frequency (GHz)	5.4272	5.3986	5.3835
(5)	Maximum frequency (GHz)	5.4446	5.4184	5.4002
	(5)–(4)	0.0174	0.0198	0.0167
(6)	Final frequency (GHz)	5.4322	5.4049	5.3840
	(5)–(6)	0.0124	0.0135	0.0162
	(6)–(4)	0.0050	0.0063	0.0005

Fig. 4. Attenuation of microwave power for rutile and anatase powders during consecutive periods of light exposure and darkness.

available trapping sites, thus facilitating an evaluation of photoresponse over greatly extended timescales. When traps are saturated, free-carrier production is in competition with carrier recombination. Because charge build-up on particles is necessarily limited, the frequency shift will eventually reach a maximum value. The curve for anatase (Fig. 3) begins to level-off after approximately 1500-s exposure, while the curve for rutile shows no evidence for this during the timescale of the exposure. When the light is switched-off, the decay of frequency apparently proceeds at a similar rate for both samples. Nevertheless, the magnitude of decrease in frequency from its maximum to final value over 1800 s is distinctly different for the two samples (see Table 2). This suggests that a greater number of free-carriers persist in the anatase sample; the higher concentration of residual free-carriers suggesting that it is the more photoactive polymorph. This premise is supported by the data for the attenuation of microwave power by the two samples during irradiation.

The absorbed microwave power (assuming constant field throughout the material under investigation) is a function of the change in the imaginary part of the complex dielectric constant. The value of the power absorption for free electrons was shown [11] to be relatively large compared to trapped

electrons, so attenuation of power corresponds largely to free-carrier production. With regard to this, Fig. 4 shows the attenuation of microwave power (A) using the same exposure profile as that used for the dF measurements. These plots follow, in real-time, the dynamics of free-carriers during consecutive periods of continuous exposure and darkness. The initial rapid production of free electrons levels-off as an equilibrium is established. The large numbers of free-carriers produced rapidly saturate traps, and though free-carrier production is in competition with recombination, it is tempered by trapping. The magnitude of conductivity measurements (and hence, attenuation of microwave power) depends on both the concentration of free-carriers produced, and their mobility. If large, comparable populations of carriers are produced, then the magnitude of conductivity values will be determined by carrier mobility. The conduction band in rutile is 0.02 eV lower than that of anatase, which indicates that there is a greater interaction of electrons with the lattice; as a result, the carriers are less mobile. This is supported by published microwave mobility measurements [10] which show much lower values for rutile (two orders of magnitude: 0.04–0.39 × 10^{-4} m^2/V s for rutile c.f. 2.3–5.1 × 10^{-4} m^2/V s for anatase). Table 2 quantifies the changes in microwave power during 1800 s of light exposure delineated in Fig. 4. The change in attenuated power for anatase is approximately twice that for rutile, this being entirely consistent with other studies that suggest the carriers in anatase are more mobile than in rutile. In addition, Fig. 4 shows that it takes longer to reach a limiting attenuated power for anatase than for rutile. It should be noted that the time taken to reach 'equilibrium' is different for power and frequency measurements since they monitor a carrier's motion at different points in its lifetime. On switching-off the light source, there is an initial further attenuation of power, suggesting that free-carriers still persist in large numbers. The attenuation of power then decays (the rate of decay being markedly different for anatase and rutile), emphasising the differences in the rates of free-carrier recombination between the samples. The more mobile carriers in anatase are able to recombine more quickly. However, the

differences between the initial power (prior to irradiation) and the value 1800 s later are 0.32 dBm and 0.18 dBm, respectively. It is possible that there are twice as many residual free-carriers remaining in the anatase sample than the rutile sample.

Combining the information gained from frequency and power measurements suggests that the anatase sample, though it produces more mobile free-carriers, possesses more traps than the rutile sample. Anatase is consequently the more photoactive material. At this point, it is extremely important to note that the photoresponse observed is not representative of anatase and rutile in general. Variables, such as crystal size, particle size and manufacturing route, give rise to subtle changes in photoactivity. The consequence of this is that a range of photoactivities will be observed for each polymorph. Indeed, it is our aim to obtain a profile of photoactivites and so establish a correlation between the underlying photophysical processes and subtle changes in the structure of TiO_2.

Along with the microwave response arising from anatase and rutile, Figs. 3 and 4 give data for a sample of mixed morphology. Time-resolved microwave conductivity studies [10] have determined the free-carrier (electron) mobility of this sample to be 0.19–0.22×10^{-4} m^2/V s, a value that is closer to (electron) mobility in rutile rather than anatase powders. Fig. 4 confirms that although mobile carriers are produced initially, their movement is rapidly restricted. This is reflected by the decrease in attenuated microwave power. The change in power after 1800-s exposure (Table 2) is only 0.02 dBm, c.f. 0.70 dBm and 0.30 dBm for anatase and rutile, respectively. On removal of the light source, attenuation of power rapidly attains a constant value. This suggests the carriers have become localised. The corresponding changes in frequency (Fig. 3) support the premise of a greater proportion of trapping sites in this sample, since the maximum frequency attained is very much less than either that of anatase or rutile. When the light is switched-off, a 'two-component' decay of frequency is seen. The initial rapid decay of frequency might imply recombination of free-carriers in anatase regions of the structure, while the much slower decay may represent recombination of trapped carriers. The net effect of these processes would be to greatly extend carrier lifetimes. This means that the sample of mixed-morphology would be highly photoactive, a proposal supported by Martin et al. [12,13]. Warman et al. [14] speculate that electrons formed in anatase microcrystallites rapidly diffuse to become localised in rutile regions and that this is consistent with the sintered cluster structure of this sample (which consists of crystallites of 30 nm which aggregate to form particles of 1 μm diameter).

Because the emphasis of this study is the application of a real-time microwave cavity perturbation technique as a gauge of the photoactivity of TiO_2 powders, a comparison with the more widely reported time-resolved techniques seems worthy. Time-resolved measurements (Figs. 5 and 6) facilitate the rapid detection of electronic events. Following a 0.5-ns pulse from an electron beam generated by a Van de Graff
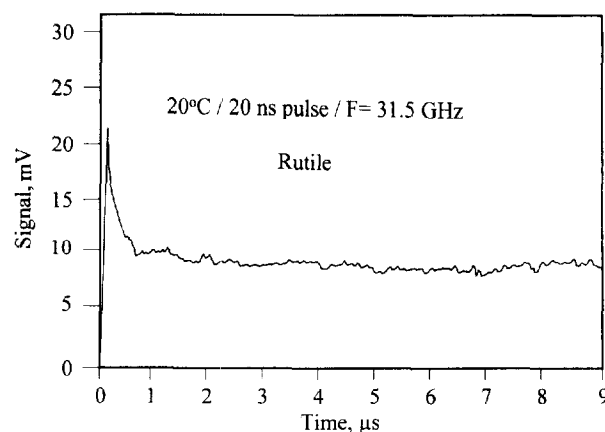

Fig. 5. Transient change in microwave conductivity (at 31.5 GHz) following pulsed irradiation (20 ns; 3 MeV) for rutile powder.
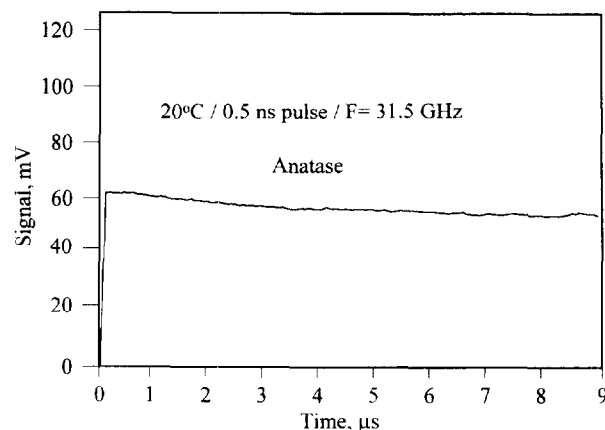

Fig. 6. Transient change in microwave conductivity (at 31.5 GHz) following pulsed irradiation (0.5 ns; 3 MeV) for anatase powder.

accelerator, the transient conductivity of anatase (62 mV) reached a significantly higher value than rutile (22 mV); though the latter exhibited a more rapid decay of conductivity. Again, this data is symptomatic of more efficient carrier-recombination in rutile, despite the greater free-carrier mobility in anatase. The data complements the real-time measurements which form the basis of this paper. Fig. 7 gives the analogous conductivity decay following a 20-ns pulse for the sample of mixed-morphology. The initial, transient conductivity (38 mV) is intermediate between the corresponding values for anatase and rutile, but the decay of the signal is greatly extended and closer to that of anatase. This further supports the conclusions derived from real-time microwave measurements, and emphasises the value of being able to monitor changes in both frequency and power.

3.2. Influence of sample mass on microwave response

Figs. 8 and 9 depict the influence of the mass of sample contained within the microwave cavity on the resonant frequency. This clearly indicates for both polymorphs that the shift is linear with mass. The magnitude of dF is much greater prior to irradiation than following 1800-s exposure to poly-
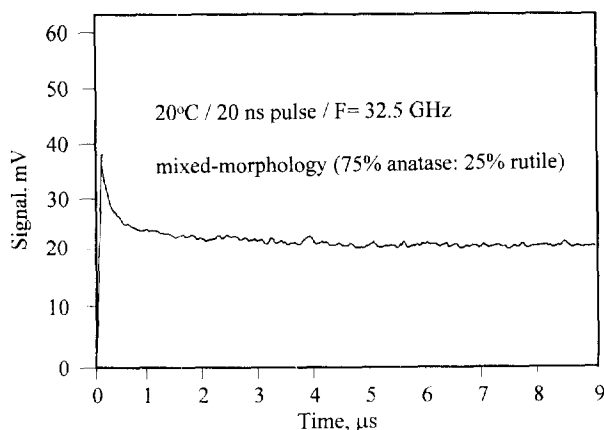
Fig. 7. Transient change in microwave conductivity (at 32.5 GHz) following pulsed irradiation (20 ns; 3 MeV) for a powder of mixed-morphology (75% anatase:25% rutile).
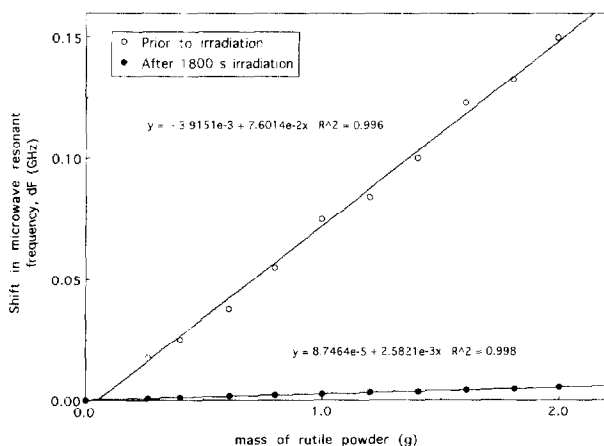

Fig. 8. Change in microwave cavity resonant frequency as a function of the mass of rutile powder held in the cavity prior to irradiation and after 1800 s of continuous, polychromatic exposure.
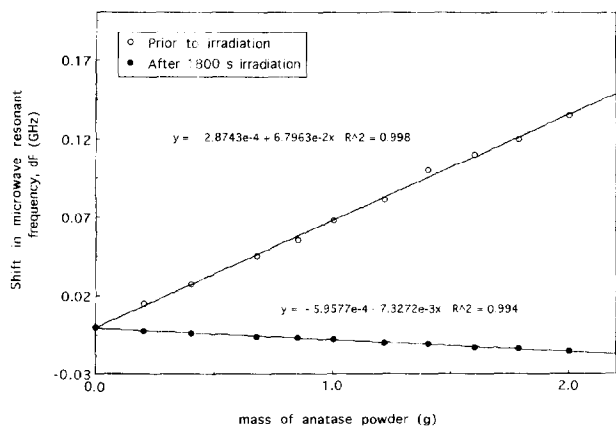

Fig. 9. Change in microwave cavity resonant frequency as a function of the mass of anatase powder held in the cavity prior to irradiation and after 1800 s of continuous, polychromatic exposure.

Fig. 10. Attenuation of microwave power as a function of the mass of anatase and rutile powders held in the cavity

chromatic light. This is consistent with the findings of Hartwig and Hinds [11] who, as stated previously, found that the magnitude of frequency shift is related to the dielectric
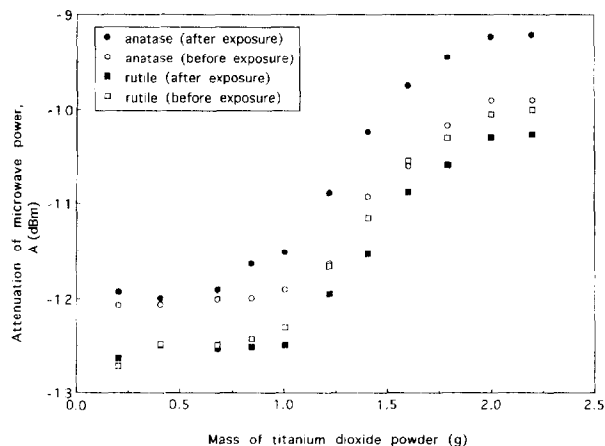
constant of the material, and that the production of free-carriers in the material decreased the dielectric constant, and so increased any shift in frequency. Linear regression on the data gave gradients of 0.068 GHz g^{-1} for anatase and 0.076 GHz g^{-1} for rutile, prior to irradiation; this being consistent with the relative difference in polarisability of the two polymorphs. After 1800-s irradiation, the gradients were -0.0073 GHz g^{-1} for anatase and -0.0026 GHz g^{-1} for rutile.

The attenuation of microwave power (Fig. 10) displayed a marked inflection ca. 1.0 g for both polymorphs. It is well-established that the power absorption is dependent on the cavity filling factor [8,11], a parameter which is defined by the microwave field distribution in the cavity and the density of the sample. For a cylindrical cavity with 'plate-like' sample (Fig. 1), the height of the dielectric in the cavity determines the amount of interaction with the electric field, assuming the sample is always distributed evenly over the cavity plate. Because the strength of the field is a maximum at the mid-height of the cavity used in this study, the sample is positioned at this point. The maximum field decreases to zero at the two ends of the cavity. Rutile and anatase powders of different crystal and particle sizes occupy different 'volumes', e.g., samples referred to as ultrafine are more 'fluffy' in nature than their larger crystal size counterparts. Clearly, optimum filling within our cavity configuration is achieved at ca. 2.0 g. Above this mass, differences in sample volume and resulting contributions from additional interactions with the field are negligible. Because response is influenced by sample density all, readings presented in this paper are derived from samples which have been packed to a fixed volume in the cavity and the readings then corrected for mass.

3.3. The influence of temperature on microwave response

Though information on the band structure of TiO_2 may be obtained by reducing temperature and then gradually increasing temperature to successively depopulate traps [15], this was not the purpose of the present study. The temperatures
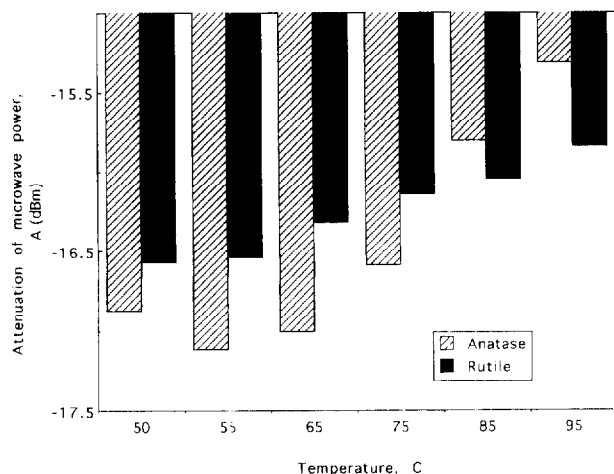
Fig. 11. Attenuation of microwave power after 1800 s of continuous, poly-chromatic irradiation for rutile and anatase powders equilibrated at 25, 50, 55, 65, 75, 85 and 95°C.
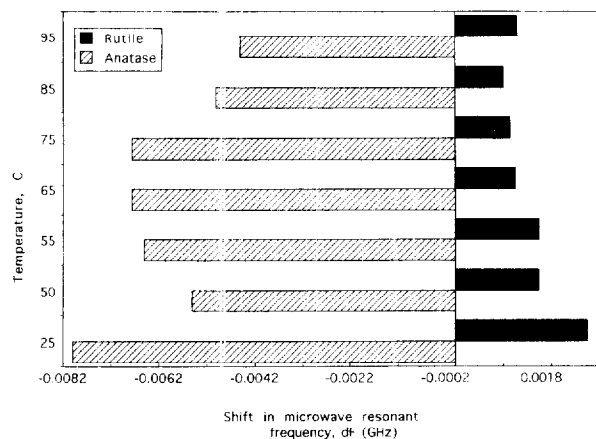

Fig. 12. Shift in microwave cavity resonant frequency after 1800 s of continuous, polychromatic irradiation for rutile and anatase powders equilibrated at 25, 50, 55, 65, 75, 85 and 95°C.

examined were relatively high and were chosen to reflect climatic variations in moderate regions, hence, the influence of temperature on microwave response.

As was expected, when samples were allowed to reach thermal equilibrium (prior to irradiation), the stored energy density of the cavity, and hence, attenuated microwave power was reduced. It must be stressed that any changes reported take into account the changes in microwave characteristics in response to physical changes in the cavity properties (thermal expansion and conductivity changes in the cavity walls). Fig. 11 illustrates the effect of increasing temperature on the attenuation of microwave power after 1800-s irradiation. For both rutile and anatase, there is a progressive decrease in attenuated power with temperature: the reduction in attenuated power being more pronounced for the anatase sample over the temperature range considered here. This effect may be attributed to increased lattice vibration, causing phonon scattering, which reduces the ability of the microwave cavity to store energy. This phenomenon is further confirmed by the changes

in resonant frequency given in Fig. 12. For both rutile and anatase, resonant frequency decreases as temperature increases. This is due to an increase in the dielectric constant arising from a greater proportion of localised carriers; increased lattice vibrations restrict the motion of free-carriers. Collectively, the data illustrate that the microwave response is sensitive to the changes in localised/delocalised carrier concentrations arising from temperature variations, and fluctuations in temperature have important consequences for the localisation and 'release' of free-carriers. In this latter respect, it would be interesting to follow the microwave response over a much wider temperature range, encompassing temperatures below 25°C. As temperature is increased from sub-ambient (e.g., 77 K), we expect an increase in free-carrier concentration as traps are successively depopulated (this should increase frequency shift and attenuation of power), at some point the contribution from lattice vibrations will become dominant (reducing frequency shift and attenuated power).

3.4. Effect of moisture on microwave response

Given the strong absorption of water in the microwave region, we might anticipate that the moisture content of TiO_2 would have a profound effect on its dielectric properties. Adsorbed water molecules are believed to react with surface bridging oxygen atoms to form hydroxyl groups [16]. The surface coverage of hydroxyl ions, resulting from chemisorbed water is known to be greater (over an equivalent surface area) for anatase than rutile [17]. Given the conjecture that adsorbed water decreases upward band bending, this would reduce the width of the depletion layer and increase carrier-recombination. A change in Fermi level by as little as 0.08 eV may result in a twenty-fold increase in the density of electrons at the particle surface. At high humidity, a thin-layer of physisorbed water [18] would give rise to a double-layer at the TiO_2–H_2O interface and the particle might function like a capacitor.

Contrasting data was obtained for the two polymorphs, after 1800 s of irradiation. This probably stems from the nature of band bending at the TiO_2 surface and the corresponding modification of charge-carrier dynamics. For anatase (Fig. 13), an increase in relative humidity caused a decrease in the shift of the cavity resonant frequency after 1800-s irradiation. This suggests that there is a reduction in free-carriers in the anatase sample at higher humidity. Rutile displayed an increase in frequency shift over an identical humidity range. This is consistent with a decrease in dielectric constant, due to an increase in free-carriers. The frequency data as a function of relative humidity fit a third order polynomial expression with a correlation coefficient of 1.00. Data for the attenuation of microwave power (Fig. 14) support the frequency data. For anatase, the attenuation of microwave power was reduced slightly with increasing relative humidity, but the opposite was observed for the rutile sample. Together, these features suggest that at higher humidity, there is more trapping in the anatase sample and accordingly, it is likely to
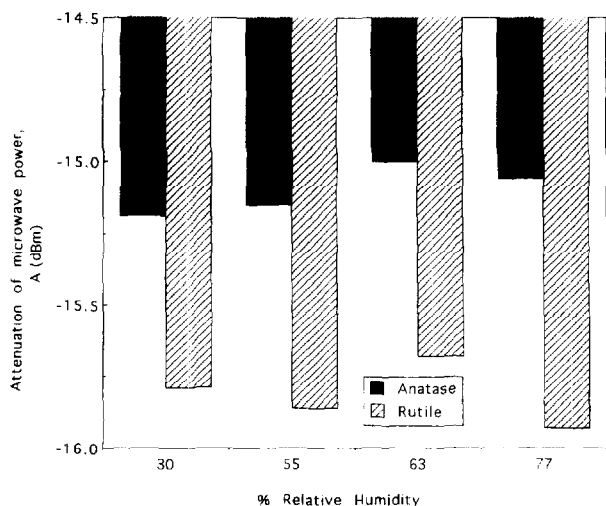
Fig. 13. Attenuation of microwave power after 1800 s of continuous, polychromatic irradiation for rutile and anatase powders equilibrated at 30, 55, 63 and 77% relative humidity.
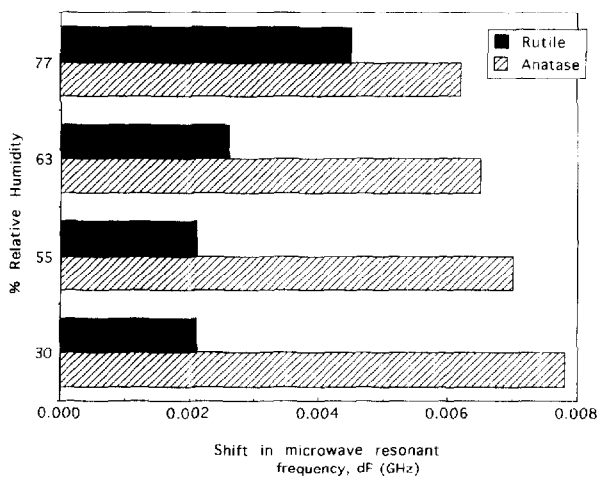

Fig. 14. Shift in microwave cavity resonant frequency after 1800 s of continuous, polychromatic irradiation for rutile and anatase powders equilibrated at 30, 55, 63 and 77% relative humidity.

be more photoactive. This is supported by practical observations related in the literature on TiO_2.

3.5. The influence of intensity and wavelength of the excitation on microwave response

To vary the intensity of the incident light, a Reflecta AF1800 projector lamp with an attached 'dimmer' unit was employed, the microwave response for equivalent amounts of uncoated rutile and anatase were measured as before, the data being summarised in Figs. 15 and 16. For anatase, as incident light intensity is increased, the shift in cavity resonant frequency is decreased, with no significant change in the attenuation of microwave power over the series. It was clear that for rutile, reducing the light intensity to 80% of the original value provided a 'cut-off' point below which changes in A or dF were negligible. Cox [18] has suggested that in

continuous wave (CW) experiments (e.g., in photocatalytic reactors [19,20]), higher light intensities raise quantum yields for fast recombination of carriers, and so, reduce quantum yields of photolysis. It is claimed that this explains why quantum efficiencies of substrate oxidation/reduction in these experiments fall as the square root of absorbed light intensity.

The use of transition metal–ion aqueous solutions as filters facilitated a preliminary investigation of the wavelength dependence of the microwave response. The wavelength(s) of light transmitted by the filters is given in Table 3. Bearing in mind the slight intensity variation over the series (Table 1), several conclusions were drawn. Fig. 17 shows a progressive decrease in the resonant frequency for rutile powders from filter 1 to filter 6, with a marked increase for filter 7 at longer wavelengths. A similar effect was observed for ana-
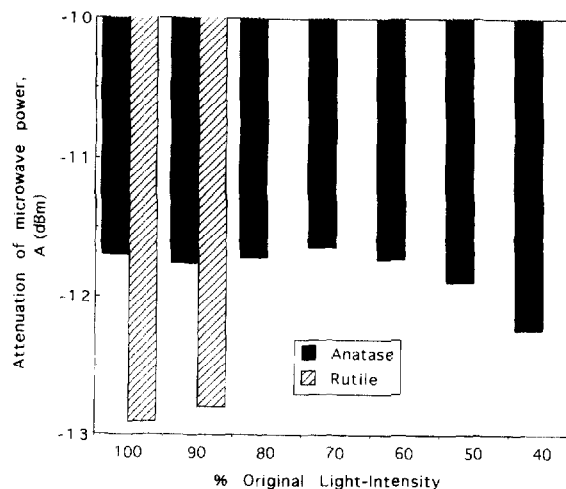

Fig. 15. Attenuation of microwave power for rutile and anatase powders after 1800-s exposure to continuous, polychromatic irradiation of specific intensity (100, 90, 80, 70, 60, 50, 40% of the original 250 W tungsten source).
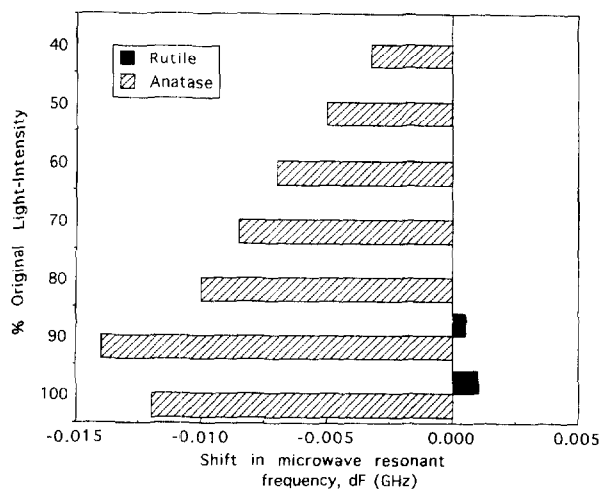

Fig. 16. Shift in microwave cavity resonant frequency for rutile and anatase powders after 1800-s exposure to continuous, polychromatic irradiation of specific intensity (100, 90, 80, 70, 60, 50, 40% of the original 250 W tungsten source).

Table 3

The specific wavelengths of the visible spectrum selected by filter solutions, from a tungsten light source (250 W)

|	Filter (aqueous solution)	Selected wavelengths
1	No filter	λs > 340 nm transmitted
2	De-ionised water	infra-red radiation removed
3	Cobalt chloride	λs between 340 and 450 nm transmitted
4	Nickel sulphate	λs between 340 and 400 nm and > 500 nm transmitted
5	Copper sulphate	λs > 350 nm transmitted
6	Chromium chloride	λs between 340 and 450 nm and 500 and 600 nm transmitted
7	Ferric chloride	λs > 500 nm transmitted
8	Potassium permanganate	λs between 400 and 500 nm transmitted
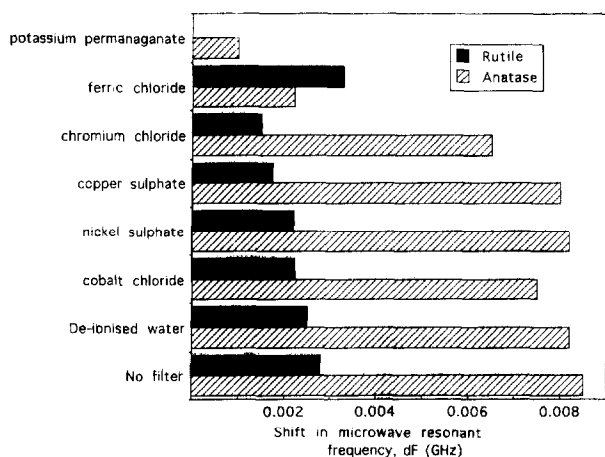
Fig. 17. Shift in microwave cavity resonant frequency for rutile and anatase powders after 1800-s continuous exposure at specific wavelengths within the visible spectrum (refer to Table 3).
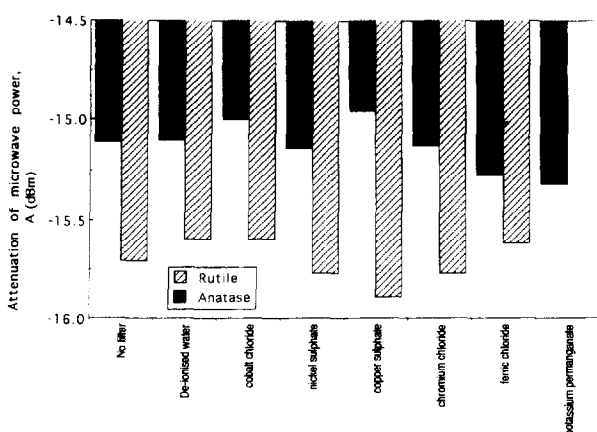

Fig. 18. Attenuation of microwave power for rutile and anatase powders after 1800-s continuous exposure at specific wavelengths within the visible spectrum (refer to Table 3).

tase, except that for filters 7 and 8, there were distinct reductions in dF. Fig. 18 gives the corresponding attenuation of microwave power for the different filters. For anatase, the

maximum power absorbed for filters that transmit light between 350–400 nm and > 500 nm, while rutile absorbs maximum power between 400 and 500 nm. The changes observed probably involve selective de-trapping from states within the bandgap (stimulated by sub-bandgap components of the incident radiation). Given the complex nature of this response, a more detailed evaluation of the wavelength dependence of pigment photoactivity is currently underway.

4. Conclusions

The use of real-time microwave measurements to follow changes in the dielectric loss and the conductivity of TiO_2 powders, when continuously irradiated with polychromatic light, has been demonstrated. Polychromatic light produces large concentrations of free-carriers that quickly saturate traps permitting the greatly extended lifetimes of carriers to be followed in real-time. The method has been demonstrated as a powerful tool enabling subtle differences in charge-carrier dynamics to be quantified. Here, sophisticated equipment does not encumber the practical aspects characteristic of the pulsed methods widely reported in the literature; though results obtained by both methods correlate. Because the technique follows changes in real-time, unlike other methods, it can follow *both* the build-up of charge-carriers during irradiation *and* their decay subsequent to irradiation. It has been demonstrated that this technique is sensitive not only to the more obvious differences between TiO_2 polymorphs, but to subtle differences in photoresponse evinced by variations in temperature, humidity, light intensity and wavelength. This allows a more precise definition of relative photoactivity. Furthermore, the flexibility of the cavity resonance approach lends itself readily to adaptation. It is possible to follow the photoactivity of TiO_2 in situ, not only in the presence of a solvent, but in a polymer matrix.

To emphasise the value of this method, in Part II of this study, the relative photoactivities of a range of commercial TiO_2 powders are predicted.

References

[1] U. Gesenhues, Double Liaison-Physique, Chemie et Economie des Peintures et Adhesifs, No. 479–480, 1996.

[2] A.L. Linsebigler, G. Lu, J.T. Yates Jr., Chem. Rev. 95 (1995) 735–758.

[3] J.M. Warman, M.P. de Haas, in: Y. Tabata (Ed.), Pulse Radiolysis, Chap. 6, CRC Press, Boca Raton, FL, 1991.

[4] I. Shih, L. Ding, S. Jatar, T.J. Pavalesk, C.H. Chanpness, Instrumentation and measurements, IM32 2 (1983) 326–331.

[5] Y. Wantanabe, J. Appl. Phys. 57 (7) (1985) 2613–2616.

[6] Y. Wantanabe, K. Maeda, S. Saito. K. Uda, Jpn. J. Appl. Phys. 16 (11) (1977) 2006–2010.

[7] G. Beck, M. Kunst, Rev. Sci. Instrum. 57 (2) (1986) 197–201.

[8] J.M. Warman, M.P. de Haas, M. Gratzel, P.P. Intelta, Nature 310 (5975) (1984) 305–306.

[9] H. Frohlich, Theory of Dielectrics: Dielectric Constant and Dielectric Loss, 2nd edn., Oxford Univ. Press, 1958.

[10] J. Warman, M.P. de Haas, P. Pichat, T.P.M. Koester, E.A. van der Zouwen-Assink, A. Mackor, R. Cooper. Radiat. Phys. Chem. 37 (1991) 433.

[11] W.H. Hartwig, J.J. Hinds, J. Appl. Phys. 40 (1969) 2020.

[12] S.T. Martin, H. Herrmann, W. Choi, M.R. Hoffmann, J. Chem. Soc., Farad. Trans. 90 (21) (1994) 3315–3322.

[13] S.T. Martin, H. Herrmann, M.R. Hoffmann, J. Chem. Soc., Farad. Trans. 90 (21) (1994) 3323–3330.

[14] J.M. Warman, M.P. de Haas, P. Pichat, N. Serpone, J. Phys. Chem. 95 (1991) 8858–8861.

[15] A.K. Ghosh, F.G. Wakin, R.R. Addiss, Phys. Rev. 184 (1969) 979.

[16] R.L. Kurtz, R. Stockbauer, T. Medey, E. Roman, J.L. Segovia, Surf. Sci. 218 (1989) 178.

[17] A.H. Boonstra, C.A.H. Amutsaers, J. Phys. Chem. 79 (16) (1975) 1694–1698.

[18] P.A. Cox, The Electronic Structure and Chemistry of Solids, Oxford Univ. Press, 1987.

[19] C. Korman, D.W. Bahnemann, M.R. Hoffmann, Environ. Sci. Technol. 25 (1991) 494.

[20] G. Irick, J. Appl. Polym. Sci. 16 (1972) 2387.